

University of Groningen

Alginate-Derived Active Blend Enhances Adsorption and Photocatalytic Removal of Organic Pollutants in Water

Vassalini, Irene; Gjipalaj, Joana; Crespi, Stefano; Gianoncelli, Alessandra; Mella, Mariella; Ferroni, Matteo; Alessandri, Ivano

Published in:
Advanced Sustainable Systems

DOI:
[10.1002/adsu.201900112](https://doi.org/10.1002/adsu.201900112)

IMPORTANT NOTE: You are advised to consult the publisher's version (publisher's PDF) if you wish to cite from it. Please check the document version below.

Document Version
Publisher's PDF, also known as Version of record

Publication date:
2020

[Link to publication in University of Groningen/UMCG research database](#)

Citation for published version (APA):

Vassalini, I., Gjipalaj, J., Crespi, S., Gianoncelli, A., Mella, M., Ferroni, M., & Alessandri, I. (2020). Alginate-Derived Active Blend Enhances Adsorption and Photocatalytic Removal of Organic Pollutants in Water. *Advanced Sustainable Systems*, 4(7), [1900112]. <https://doi.org/10.1002/adsu.201900112>

Copyright

Other than for strictly personal use, it is not permitted to download or to forward/distribute the text or part of it without the consent of the author(s) and/or copyright holder(s), unless the work is under an open content license (like Creative Commons).

The publication may also be distributed here under the terms of Article 25fa of the Dutch Copyright Act, indicated by the "Taverne" license. More information can be found on the University of Groningen website: <https://www.rug.nl/library/open-access/self-archiving-pure/taverne-amendment>.

Take-down policy

If you believe that this document breaches copyright please contact us providing details, and we will remove access to the work immediately and investigate your claim.

Downloaded from the University of Groningen/UMCG research database (Pure): <http://www.rug.nl/research/portal>. For technical reasons the number of authors shown on this cover page is limited to 10 maximum.

Alginate-Derived Active Blend Enhances Adsorption and Photocatalytic Removal of Organic Pollutants in Water

Irene Vassalini,* Joana Gjipalaj, Stefano Crespi, Alessandra Gianoncelli, Mariella Mella, Matteo Ferroni, and Ivano Alessandri*

The ever-increasing need for clean water is one of the most urgent sustainable development goals, which requires environmentally-friendly strategies for water remediation against different types of pollutants. In this work, the possibility of using alginate, a biocompatible and natural polysaccharide, is explored for the preparation of both oxide (TiO₂, Al₂O₃, and yttria-stabilized ZrO₂ (YSZ)) macrobeads and an active blend of rich carbon nanoparticles, depolymerized alginate, formic acid, and a complex mixture of other organic acids. In particular, the active blend is obtained through low-energy-demanding microwave assisted digestion of sodium alginate solution, and it is used to enhance the decontamination activity of oxide macrobeads in mild conditions (e.g., low temperature, no pH buffers, and visible illumination). It is demonstrated that the alginate-derived active blend obtained without the addition of any other chemicals increases primarily the adsorption capability of oxide macrobeads toward positively charged pollutants (methylene blue, crystal violet, and tetracaine) and, also, the photocatalytic activity of TiO₂ during their degradation. Interestingly, functionalization with the obtained alginate-derived active blend enables better performance in comparison with functionalization of its single components or with carbon-dots (C-Dots) obtained with conventional and more energy-demanding hydrothermal methods, enabling them to obtain a fully sustainable, environmentally-friendly system for water remediation.


1. Introduction

Finding new strategies for catalytic purposes^[1,2] and, in particular, for the simultaneous removal of different types of pollutants^[3] (dyes, metallic ions, pharmaceuticals, pesticides, personal care products, and antibiotics) is fundamental to respond to the ever-increasing needs of clean water and soils. In fact, if in developing countries, the problem of high concentration of dyes in wastewater is still present because of the high activity of textile industry; in Europe and USA, the problem of the so-called emerging pollutants, among which pharmaceutical compounds are of particular interest, is becoming predominant. This category of chemicals lacks for a clear legislation and, in many cases, their effects on human health are still unknown. Moreover, their detection can be extremely challenging. In this context, the materials utilized for decontamination should be simultaneously stable over a long-time, nontoxic, easily recovered, and characterized by high efficiency (good adsorption, fast

Dr. I. Vassalini, Prof. M. Ferroni, Prof. I. Alessandri
INSTM (Research Unit of Brescia)
CNR-INO (Unit of Brescia)
Department of Information Engineering
University of Brescia
via Branze 38, Brescia 25123, Italy
E-mail: irene.vassalini@unibs.it; ivano.alessandri@unibs.it

Dr. J. Gjipalaj
Department of Environmental Engineering
Faculty of Civil Engineering
Polytechnic University of Tirana
Rruga Muhamet Gjollështa Nr. 54, Tirana 1023, Albania

Dr. S. Crespi
Stratingh Institute for Chemistry
University of Groningen
Nijenborgh 4, Groningen 9747 AG, The Netherlands

 The ORCID identification number(s) for the author(s) of this article can be found under <https://doi.org/10.1002/adsu.201900112>.

Dr. A. Gianoncelli
INSTM (Research Unit of Brescia)
Department of Molecular and Translational Medicine
University of Brescia
Viale Europa 11, Brescia 25123, Italy

Prof. M. Mella
Department of Organic Chemistry
University of Pavia
Via Taramelli 12, Pavia 27100, Italy

Prof. M. Ferroni
CNR-IMM
Bologna Section, via Gobetti 4, Bologna 40129, Italy

DOI: 10.1002/adsu.201900112

pollutant degradation, and formation of nonhazardous byproducts) against different types of pollutants. Besides, the ideal decontaminant should be obtained through an environment-friendly synthesis, using low-impact reactants and protocols. Combining all these aspects is a grand challenge in the design of materials for environmental remediation. For example, activated carbon, the conventionally employed adsorbent, is characterized by expensive and highly energy-demanding processes of production and thermal regeneration (500–900 °C). On the other hand, TiO₂ nanoparticles (NPs), which are characterized by high photocatalytic activity under UV illumination, are affected by several limitations in terms of longevity, adsorption capability, stability, risk of nanotoxicity, and recovery.^[4,5] We have recently demonstrated that these drawbacks, which are ultimately related to nanostructuring, can be overcome by alginate-assisted ionotropic gelation of TiO₂ nanopowders, which result in the formation of millimeter-sized porous TiO₂ macrobeads made of stabilized NPs.^[6] Ionotropic gelation proceeds through ionic cross-linking between a polyelectrolyte solution containing oxide nanopowders and a solution of the suitable counterion. In particular, Ca²⁺ ions are utilized for the cross-linking solution, and alginate, which is a nontoxic, biodegradable, and naturally occurring polysaccharide extracted from brown seaweed, was chosen as the gelling agent, because of its excellent biocompatibility, safety, and cheapness.^[7–10] Macrobeads maintain the high photocatalytic activity of TiO₂ NPs, with additional benefits related to their easy and fast recovery by sedimentation (avoiding the need of further centrifugation or filtering steps), high surface area, and porosity.

The same synthetic procedure can be extended to the preparation of macrobeads based on other oxides, such as Al₂O₃ and yttria-stabilized ZrO₂ (YSZ). In all those cases, alginate contributes to increased adsorption capability of the macrobeads toward aqueous pollutants, especially thanks to the presence of negatively charged hydroxyl and carboxylate functional groups in its internal structure.^[10–12] However, in this respect, the performances of macrobeads are still lower than that of conventional adsorbents, like activated carbon. On the other hand, activated carbon per se cannot be utilized for photocatalysis. For those reasons, developing photocatalytic macrobeads with increased adsorption of pollutants would be a significant step forward in the field of water remediation.

In recent years carbon-dots (C-Dots) have been proposed as alternative co-catalysts that can be combined with adsorbents^[13,14] or photocatalysts^[15–23] for water remediation. C-Dots are particularly attractive from a circular economy perspective since, in addition to conventional sources (graphite,^[21] graphene,^[18] carbon nanotubes,^[24] or purified charcoal^[24]), a large variety of precursors can be obtained from natural sources, such as alginate,^[25,26] glucose,^[17,20] fructose,^[19] orange peel,^[27] tea,^[28,29] olive pit,^[30] egg white,^[31] ascorbic acid,^[32] citric acid,^[23] chitosan,^[33] or lignocellulose,^[34] which can be easily recovered from food and organic waste.

However, the production of C-Dots is typically carried out in hydrothermal reactors for several hours and often involves the use of organic passivating agents (e.g., amines) or strongly oxidizing agents (e.g., nitric acid and H₂O₂). Moreover, although the size of C-Dots is a key factor for controlling their optical properties,^[35] which are relevant for sensing^[36] and biomedical

applications,^[37] its role in photocatalysis and in pollutant adsorption is not straightforward as for other, more conventional, catalysts.^[22] In fact, most of the activity could be related to the molecular moieties that passivate the dots.^[38,39] Gaining more insights into the photocatalytic activity of C-Dots and developing truly sustainable alternative strategies to maximize adsorption/removal of pollutants in groundwater are two main challenges in the field of environmental remediation.^[40]

In this work, we explore the possibility of taking advantage of the excess of the alginate solution utilized for ionotropic gelation of oxide powders as a precursor for preparing a pollutant-capturing blend that can be utilized for functionalizing oxide macrobeads, making them more efficient in removing different types of pollutants from water. The active blend, consisting of a complex mixture of depolymerized alginate, organic acids, and carbon-based nanoparticles (C-NPs), was obtained by treating the alginate in a 150 W microwave (MW) digester reactor for only 15 min according to a new procedure, without any additional oxidizing agents or acids. This route reduces energy consumption, synthesis time, and purification steps of previously reported procedures for the preparation of C-Dots, improving the environmental sustainability of the whole production process.

The performances of the oxide macrobeads functionalized with the alginate-derived active blend in the removal (adsorption and photodegradation) of different types of pollutants (organic dyes: i.e., methylene blue (MB), crystal violet (CV), and methyl orange (MO); different pharmaceuticals: diclofenac and tetracaine) were assessed and compared with those of C-Dots obtained from alginate by a conventional hydrothermal route. The main factors that control the adsorption mechanism were in-depth investigated.

In particular, we demonstrated that the functionalization with the alginate-derived active blend is a universal strategy to enhance the adsorption capability of oxide macrobeads toward positively charged pollutants. In the case of TiO₂ macrobeads, the functionalization strongly improves the adsorption of pollutants and enables fast water decontamination under not only UV illumination, but also direct solar irradiation, in mild and real-working conditions.

2. Results and Discussion

The main objective of this work is the preparation of innovative systems, which are able to combine adsorption and degradation capabilities toward different types of pollutants in mild conditions, avoiding the use of additional chemicals, high temperature, or complex setups. In addition to simple working conditions, it is fundamental that their synthesis could be performed through simple and environmental-friendly procedures. In order to meet all these requirements, we prepared oxide (TiO₂, Al₂O₃, and yttria-stabilized ZrO₂) macrobeads through ionotropic gelation, by combining the corresponding commercial oxide powders with alginate, as reported in the “Experimental Section.” The results are spheroidal macrobeads characterized by an irregular morphology with an average diameter of 0.6 ± 0.1 mm for Al₂O₃, 0.9 ± 0.1 mm for TiO₂, and 0.8 ± 0.2 mm for YSZ. On the surface of the different beads, we

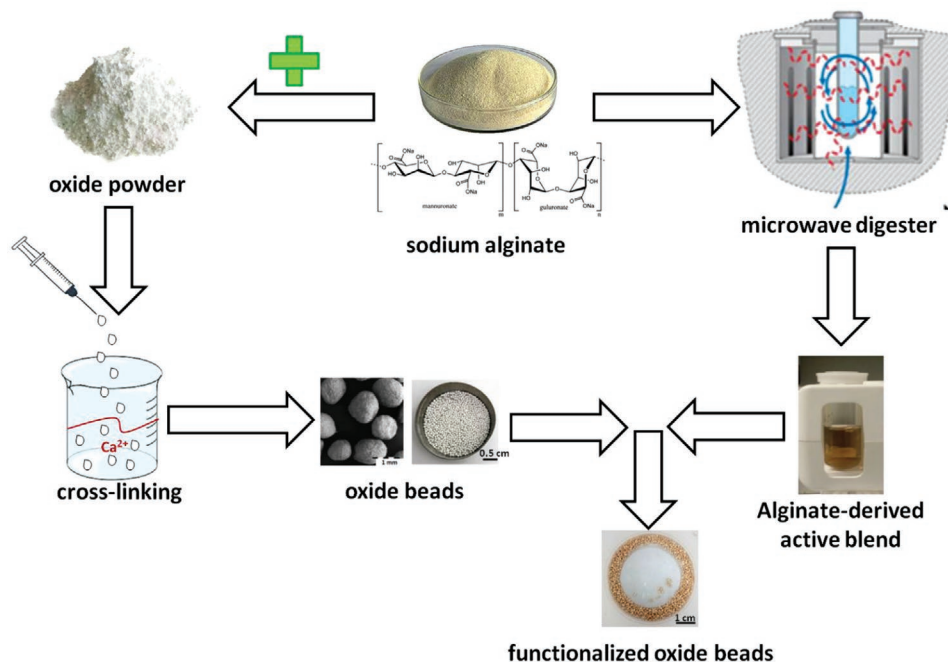


Figure 1. Scheme of the preparation of oxide beads and functionalized oxide beads using sodium alginate, both as the gelling agent and precursor for a complex active blend containing C-NPs.

can observe the presence of small mounds and ribbings, which are due to the formation of an elongated droplet through the syringe needle used for their preparation and make their shape strongly dependent on the applied pressure to the syringe and on the drop height. All the beads are characterized by high surface roughness, originated from the tightly packed grains of the oxide powders, and high porosity ($\approx 70\%$), resulted from the drying of the alginate-oxide hydrogels. Hg-porosimetry measurements revealed a monomodal pore size distribution for Al_2O_3 and YSZ, with an average pore diameter of 80 nm for Al_2O_3 and 100 nm for YSZ, while a bimodal pore size distribution is measured for TiO_2 beads, with two maxima located at about 30–40 and 800–900 nm (Figure S1a–c, Supporting Information).

In this work, alginate has been used also as source for the preparation of complex solution containing C-NPs through microwave digestion, according to a novel procedure, working at $T = 200^\circ\text{C}$, $p = 200$ bar, and power = 150 W for 15 min. After the thermal treatment of 0.9 mg mL^{-1} alginate solution in water, an orange-brownish solution (alginate-derived active blend) is obtained, and it has been used to functionalize the oxide beads (Figure 1).

The alginate-derived active blend has been characterized in terms of UV–vis absorption, light photoemission, chemical composition (IR, Raman, and NMR spectroscopy), and morphology. The UV–vis spectrum (Figure S2a, Supporting Information) is characterized by an intense broad peak centered at around 300 nm, ascribed to the presence of multiple energy absorbing residues upon the C-NPs surface and to $\pi \rightarrow \pi^*$ electron stacking transition of aromatic sp^2 domains.^[18,21,24,27] When irradiated with a UV lamp emitting at 365 nm, blue photoluminescence is recorded (Figure S2b, Supporting Information).

To obtain insights into the chemical composition of the alginate-derived active blend, the Fourier transform infrared spectroscopy, Raman, and NMR spectra of the solution have been recorded (Figure 2).

The bends in the IR spectrum (Figure 2a) centered at 1597 and 1400 cm^{-1} (due to asymmetric and symmetric stretching of C–O–O of carboxylate) and the peaks at 1110–1060 cm^{-1} (due to C–O–C and C–C stretching vibrations of the pyranose rings, with contribution from C–C–H and C–O–H deformations) demonstrated that the solution inherited most of the functional groups from the original material. The broad bend centered at 3380 cm^{-1} , instead, is caused by –OH vibrations. Anyway, as reported by Ren and co-workers,^[41] the intensity ratio of the peak at $\approx 1100\text{ cm}^{-1}$ typical of C–O–C stretching to the peak at $\approx 1600\text{ cm}^{-1}$ due to C–O–O of carboxylate can be used to monitor the depolymerization of alginate, with a higher value typical of more destructured alginate. In our experiment, T_{1095}/T_{1606} is equal to 1.04 in the case of alginate, while it increases to $T_{1109}/T_{1597} = 1.17$ in the case of the alginate-derived active blend. The Raman spectrum (Figure 2b) is characterized by the presence of two peaks at 1370 and 1550 cm^{-1} , corresponding to the D and G bands, respectively, typical of carbonaceous species. The D band is ascribed to disordered sp^2 carbons, while the G band arises from the in-plane stretching vibration mode E_{2g} of crystalline graphite carbons. The ratio of the intensities (I_D/I_G) of these two Raman bands can be used to study the structural properties of the carbon framework, in particular, the degree of crystallinity and relative abundance of core carbon atoms versus surface atoms. In this case, the I_D/I_G is equal to 0.9, indicating more abundant graphitic atoms; in addition, the D band is very broad and not well defined, indicating the presence of a not completely destructured carbonaceous form. Performing the microwave digestion

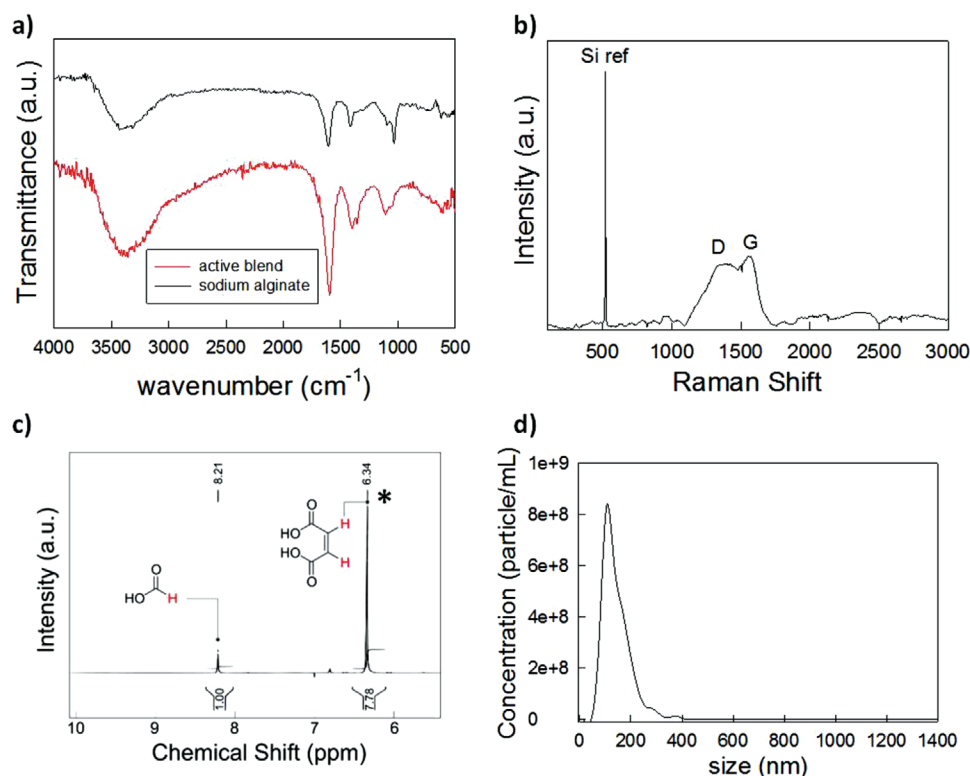


Figure 2. Characterization of alginate-derived active blend. a) IR spectrum, b) Raman spectrum. c) NMR spectrum using as internal standard (*) maleic acid, and d) hydrodynamic radius of contained C-NPs.

in D_2O allows us to follow the course of the reaction through NMR spectroscopy (Figure 2c). A signal attributed to the formation of formic acid appears at 8.21 ppm, leading to the conclusion that the alginate has not been completely converted into carbon. Quantitative NMR analysis conducted using maleic acid as internal standard (found at 6.34 ppm) affords to determine a concentration of 0.0023 M in formic acid after microwave treatment, equal to the half of the concentration of the starting alginate solution. In the NMR spectrum, other minor peaks are visible, but their interpretation results nontrivial, leading to the conclusion that during the digestion treatment a complex mixture of organic acids and depolymerized alginate is formed.^[42,43] Nonetheless, the formation of nanoparticles has been confirmed by means of Nanoparticle Tracking Analysis (NTA, Nanosight300), which confirms the presence in the suspension of nanoparticles with an average hydrodynamic radius of 143 ± 2 nm (Figure 2d) that are embedded inside the alginate-derived matrix, as confirmed by transmission electron microscopy (TEM) analysis (Figure S3, Supporting Information).

The alginate-derived blend has been used to functionalize the oxide microbeads synthesized through ionotropic gelation. The functionalization has been performed by simply mixing 300 mg of oxide beads in 3 mL of alginate-derived blend for 60 min, after which the beads have been removed from the solution and are left to dry in open air and at room temperature for, at least, 12 h. The functionalization has been confirmed by the change of color of the beads from white to orange (Figure 1).

As a starting point, the capability of water remediation of both oxide beads and functionalized oxide beads has been

determined using methylene blue (6.5×10^{-6} M solution), which has been chosen as the model cationic dye.

As shown in Figure 3a, the functionalization with the alginate-derived blend enables to enhance the adsorption capability of all the oxide beads. In fact, the percentage of methylene blue adsorbed at dark after 90 min of mixing with the substrate after the functionalization changes from 20% to 77% in the case of Al_2O_3 , from 27% to 74% in the case of YSZ, and from 23% to 82% for TiO_2 . Even if the functionalization with alginate-derived blend does not enable to reach a complete MB adsorption as in the case of activated carbons, it can be identified as a universal strategy to improve the adsorption capability of different oxides.

In all the reported cases, the adsorption of MB on macrobeads can be approximated through a pseudo-second-order isotherm (Figure 3b), suggesting that the functionalization of oxide beads with the alginate-derived blend does not modify the MB adsorption mechanism. This mechanism is based on chemical and electrostatic interactions between negatively charged groups adsorbed on the surface of the oxide beads and positively charged MB^+ species in solution,^[10,12] as described later.

In the case of TiO_2 , by means of functionalization with alginate-derived blend, it is possible to achieve an additional improvement of decontaminant performances. In fact, an enhancement of the photodegradation activity is recorded; the UV irradiation time needed to obtain complete removal of MB is reduced from 75 to 30 min (Figure 3c). For comparison, the self-degradation of MB under UV illumination has been

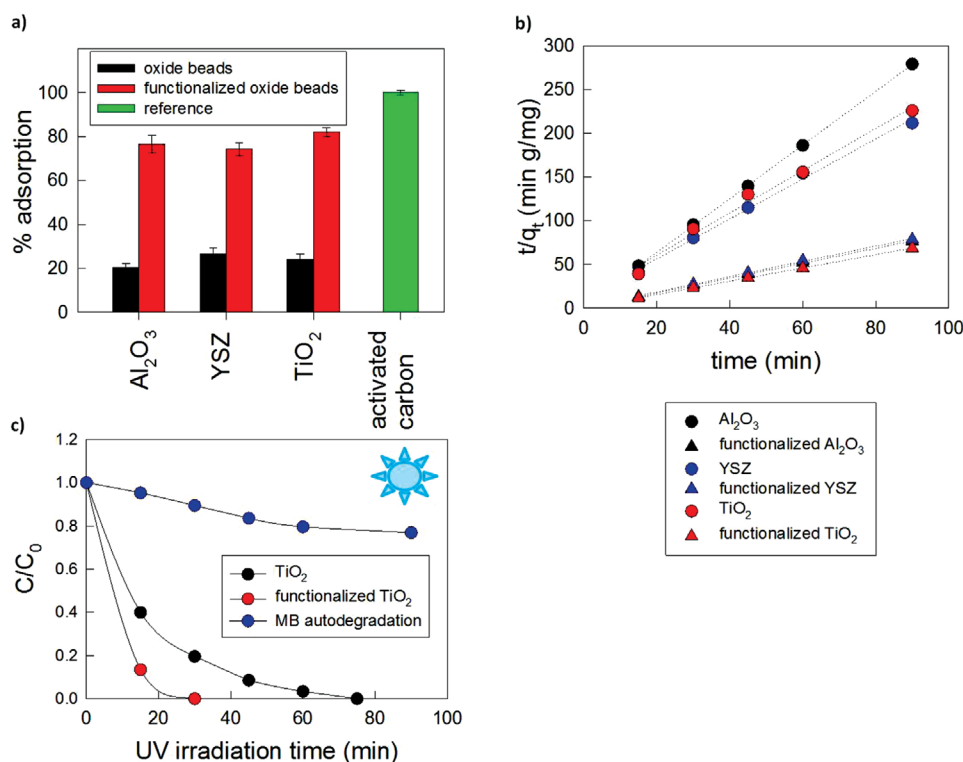


Figure 3. a) Comparison between the absorption capability of MB 6.5×10^{-6} M of Al_2O_3 , YSZ, and TiO_2 beads before (black) and after (red) functionalization with alginate-derived active blend. As reference, activated carbons have been used. b) Pseudo-second-order isotherms of Al_2O_3 , YSZ, and TiO_2 beads before (circles) and after (triangles) functionalization with alginate-derived active blend during the adsorption in dark of MB 6.5×10^{-6} M solution. c) Comparison between the photodegradation activity under UV illumination of TiO_2 beads before and after functionalization. MB autodegradation under UV light has been added as reference. Error bars within the experimental point size.

calculated by evaluating the variation of MB concentration over the time under UV light; after 90 min of irradiation, the self-degradation is limited to the 20% (Figure 3c). On the other hand, neither Al_2O_3 nor YSZ is able to promote photodegradation, and functionalization does not stimulate photocatalysis (Figure S4, Supporting Information).

Since in the case of TiO_2 it is possible to combine adsorption and photodegradation, TiO_2 beads have been selected and used for further functional characterization and to investigate the reasons at the basis of the improvement of decontamination properties by means of functionalization with the alginate-derived blend.

First of all, a comparison between alginate-derived active blend synthesized with the here-proposed novel method based on the use of a digester and C-Dots synthesized employing a hydrothermal treatment of alginate with H_2O_2 (H_2O_2 C-Dots) as reported by Zhou et al.^[25] has been performed. Figure 4a shows that the C-NPs-rich blend synthesized through the novel heat treatment of alginate with the digester enables to obtain functionalized oxide macrobeads characterized by a higher absorption capability ($\pm 10\%$), in comparison to H_2O_2 C-Dots (MB adsorption is equal to 82% for alginate-derived blend and 71% for H_2O_2 C-Dots). Probably the co-presence of depolymerized alginate, formic acid, and a mixture of organic acids inside the suspension of C-NPs enhances the affinity of the adsorbing system toward MB. As regards the photodegradation activity under UV illumination, instead, the two types of alginate-

derived suspensions do not show any significant difference, and both of them are equally able to improve the TiO_2 macrobeads performances (Figure 4b). We estimated the energy consumption for the two synthetic procedures: for the H_2O_2 C-Dots 30 240 kJ is needed, while for the alginate-derived active blend 135 kJ is enough. Ultimately, the here-proposed novel treatment of sodium alginate with the microwave digester is an environment-friendly procedure for the preparation of active C-NP-rich solution, as it does not involve any harmful reactants (no acids or oxidizing reagents) and requires a limited amount of energy.

In order to have a deeper insight into the decontamination process, we have compared the performances of blend-functionalized TiO_2 beads with those of TiO_2 beads, alginate-functionalized TiO_2 beads, and formic-acid-functionalized beads. Alginate-functionalized TiO_2 beads have been obtained by mixing 3 mg of TiO_2 beads with 3 mL of alginate solution 0.0045 M (solution of sodium alginate with the same concentration of that used for the microwave synthesis of the blend), while formic-acid-functionalized beads have been obtained by mixing 3 mg of TiO_2 beads with 3 mL of formic acid 0.0045 M (solution of formic acid with the same concentration of that of sodium alginate used for the synthesis of the blend) or 0.0023 M (solution of formic acid with the same concentration of that of formic acid determined by NMR spectroscopy inside the blend). These concentrations of formic acid and sodium alginate have been chosen in order to verify if the microwave treatment with the digester

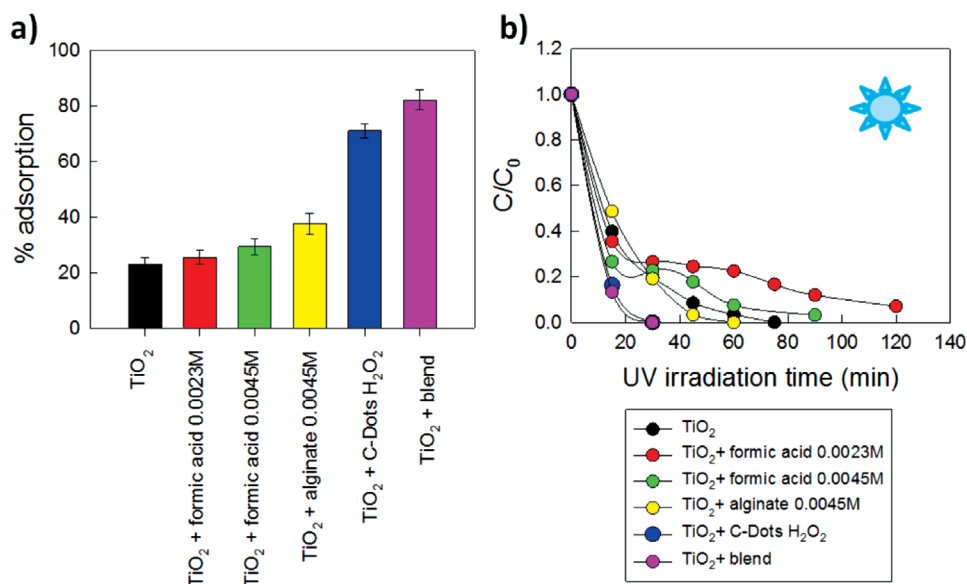


Figure 4. a) Comparison between the absorption capability of TiO₂ beads functionalized in different ways. b) Comparison between the photodegradation activity under UV illumination of TiO₂ beads before and after different types of functionalization. MB 6.5×10^{-6} M solution has been used as model pollutant. Error bars within the experimental point size.

enables to obtain an added value in comparison to the simple immersion of the beads into alginate or formic acid solutions. The obtained results are summarized in Figure 4. As shown in Figure 4a, the adsorption capability of TiO₂ beads is only slightly enhanced in the case of functionalization with formic acid (percentage absorption of $\approx 23\%$ in the case of formic acid 0.0023 M and $\approx 30\%$ in the case of formic acid 0.0045 M, which is 1.3 times the percentage absorption of not functionalized TiO₂ beads) or not-treated alginate solution (percentage absorption of $\approx 38\%$, which is 1.65 times the percentage absorption of not functionalized TiO₂ beads), while it is possible to enhance the TiO₂ adsorption capability of 3.5 times in the case of alginate solution treated with microwave digestion (i.e., alginate-derived blend). In terms of photodegradation (Figure 4b), the best results are obtained in the case of functionalization with alginate solution treated with microwave digestion (i.e., alginate-derived blend). In fact, in the case of functionalization with not-treated alginate solution only a slight lowering of irradiation time (60 min instead of 75 min) is recorded, while the irradiation time increases in the case of functionalization with formic acid (more than 120 min for formic acid 0.0023 M and 90 min for formic acid 0.0045 M, while 75 min is enough for plain TiO₂ beads). On the contrary, in the case of functionalization with microwave-treated alginate solution, the irradiation time is reduced by 2.5 times. From these results, it is clear that the treatment of the alginate solution with the microwave digester is fundamental to create a complex matrix of organic acids, depolymerized alginate and C-NPs, which optimizes the performances of TiO₂ during decontamination and which enables us to obtain better performances in comparison to those of all the single components.

Second, the parameters influencing the decontamination process, such as pH and the amount of adsorbent per milliliter of pollutant solution, have been investigated.

Three different pH values were considered: 1.5, 6.5, and 11.5. As visible in Figure 5a, adsorption is strongly affected by the solution pH. Considering not functionalized TiO₂ macrobeads, at pH = 1.5 the adsorption of MB is limited at $\approx 12\%$, which increases to $\approx 25\%$ when pH is equal to 6.5 and to $\approx 32\%$ when pH is 11.5. The lower adsorption in strongly acidic environment is justified by the fact that at pH < 6.2 (the point of zero charge of Hombikat anatase powder^[6]) TiO₂ is characterized by a positive surface charge, which does not promote the adsorption of positively charged species (such as MB in water solution). On the contrary, increasing the pH of the solution, the surface charge of TiO₂ becomes more negative, facilitating the MB⁺ adsorption. A similar trend is also observed in the case of functionalized TiO₂ macrobeads; MB adsorption is penalized in acidic environment (the percentage adsorbed at pH 1.5 is limited to $\approx 39\%$ instead of 82% at pH 6.5 and 11.5). This fact suggests that the functionalization does not modify the adsorption mechanism, as confirmed by the adsorption isotherms (Figure 3b). In fact, also after functionalization with alginate-derived blend, MB adsorption occurs through electrostatic attraction between positively charged MB in solution and negatively charged adsorbent surface. Interestingly, increasing the pH from 6.5 to 11.5 after functionalization does not enhance the adsorption capability of the system, probably because at pH 6.5, the surface is already more negative (thanks to the alginate-derived functional groups) and there is no significant variation of surface charge of the functionalized TiO₂ at the two values of pH. It is worth noting that even if a more acidic environment reduces MB adsorption, functionalized TiO₂ beads at pH 1.5 adsorb a higher percentage of MB in comparison to the nonfunctionalized counterparts at the optimized condition (pH 11.5). This fact suggests that in the case of macrobeads functionalized with the alginate-derived blend, in addition to electrostatic attraction, intermolecular interactions between molecules contained in the solution used for functionalization and the pollutant play a key role in adsorption.

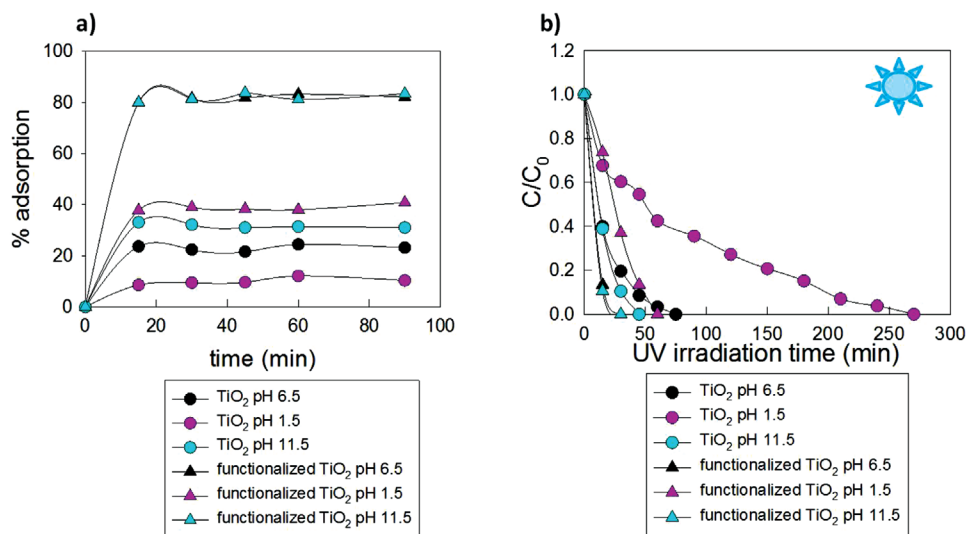


Figure 5. a) Percentage of adsorbed methylene blue (MB 6.5×10^{-6} M solution) by TiO₂ beads and TiO₂ beads functionalized with alginate-derived blend in the presence of different values of solution pH. b) UV photodegradation activity of TiO₂ beads and TiO₂ beads functionalized with alginate-derived blend during the degradation of MB 6.5×10^{-6} M solution at different values of solution pH. Error bars within the experimental point size.

As regards photodegradation (Figure 5b), a similar pH dependence is observed for both functionalized and plain TiO₂ macrobeads; it is quicker in the case of pH = 11.5, followed by the system at pH = 6.5 and slower in the case of pH = 1.5. Probably this is caused by the fact that photodegradation occurs through a mechanism based on the formation of OH[•] radicals, which is facilitated in alkaline environment.

However, we decided to operate in nearly neutral pH, without any external addition of base/acid, in order to assess the potential use of these materials for real-world application. In these conditions (pH 6.5), the experimental surface charge of TiO₂ macrobeads is equal to -12.9 ± 0.2 mV, and becomes -15.6 ± 0.3 mV upon functionalization with the alginate-derived active blend, which confirms the hypothesis discussed above.

Further studies have been performed on MB 6.5×10^{-6} M solution in mineral water (chemical analysis in Figure S5a in the Supporting Information). As shown in Figure S5b (Supporting Information), the presence of additional ions (both positive and negative) in mineral water does not interfere in the MB adsorption capability of TiO₂ and functionalized TiO₂ beads. On the contrary, passing from Milli-Q to mineral water, a slight increase in MB adsorption (23% vs 28% for TiO₂ beads and 82% vs 83% for functionalized TiO₂ beads) is recorded. An additional reduction in UV illumination time (75 vs 45 min for TiO₂ beads and 30 vs 15 min for functionalized TiO₂ beads) is observable (Figure S5c, Supporting Information). Probably these effects are due to an increase of the solution pH.

Moreover, we have investigated the effect of variation of the amount of TiO₂ beads per unit volume of MB solution and the recyclability of our substrates. Three different concentrations of adsorbent have been considered: 25, 50, and 100 mg mL⁻¹. As visible in Figure S6 (Supporting Information), MB adsorption percentage increases with the increase of the amount of adsorbent, passing from $\approx 12\%$ in the case of TiO₂ 25 mg mL⁻¹ to $\approx 16\%$ in the case of TiO₂ 50 mg mL⁻¹ and to $\approx 23\%$ in the case of TiO₂ 100 mg mL⁻¹. Photodegradation, instead, is not

significantly affected by the concentration of TiO₂. For further studies, we decided to set the concentration of TiO₂ to 100 mg mL⁻¹. As regards the recyclability, the activity of TiO₂ and functionalized TiO₂ macrobeads was tested over three consecutive cycles. As visible from Figure S7a (Supporting Information), recycling enables us to slightly enhance the MB adsorption percentage of nonfunctionalized TiO₂ from 24% (first cycle) to 40% (third cycle), probably because of the presence of organic residues that accumulate on the TiO₂ surface after each use, which improve the affinity toward MB. On the contrary, recycling slightly reduces the MB adsorption percentage of functionalized TiO₂ (passing from 82% for the first cycle to 70% for the third cycle). It is probably due to a small leaching of the active blend from the macrobeads' surface during the test, which anyhow does not compromise their activity, since functionalized macrobeads at the third cycle of activity are still more effective than nonfunctionalized TiO₂. A similar, but less regular, trend can be observed during photodegradation experiments: recycling improves the performances of nonfunctionalized TiO₂, while reduces those of functionalized macrobeads (Figure S7b,c, Supporting Information).

In order to verify the possibility of using TiO₂ beads functionalized with alginate-derived blend as universal substrates for water remediation, their performances were evaluated during the removal of different organic dyes. In addition to methylene blue (6.5×10^{-6} M), crystal violet (CV, 5×10^{-6} M) and methyl orange (MO 6.5×10^{-6} and 5×10^{-5} M) were tested. As visible from Figure 6a, TiO₂ beads are very effective in the adsorption of CV (even more than in the case of MB), while adsorption of MO is limited to 15%.

These adsorption behaviors can be interpreted again on the basis of electrostatic interactions between negatively charged TiO₂ surface (at pH 6.5, the surface charge of TiO₂ beads is -16 ± 1 mV) and positively charged and CV⁺ or negatively charged MO⁻ ions in solution. It is interesting to notice that this effect is emphasized by the functionalization with

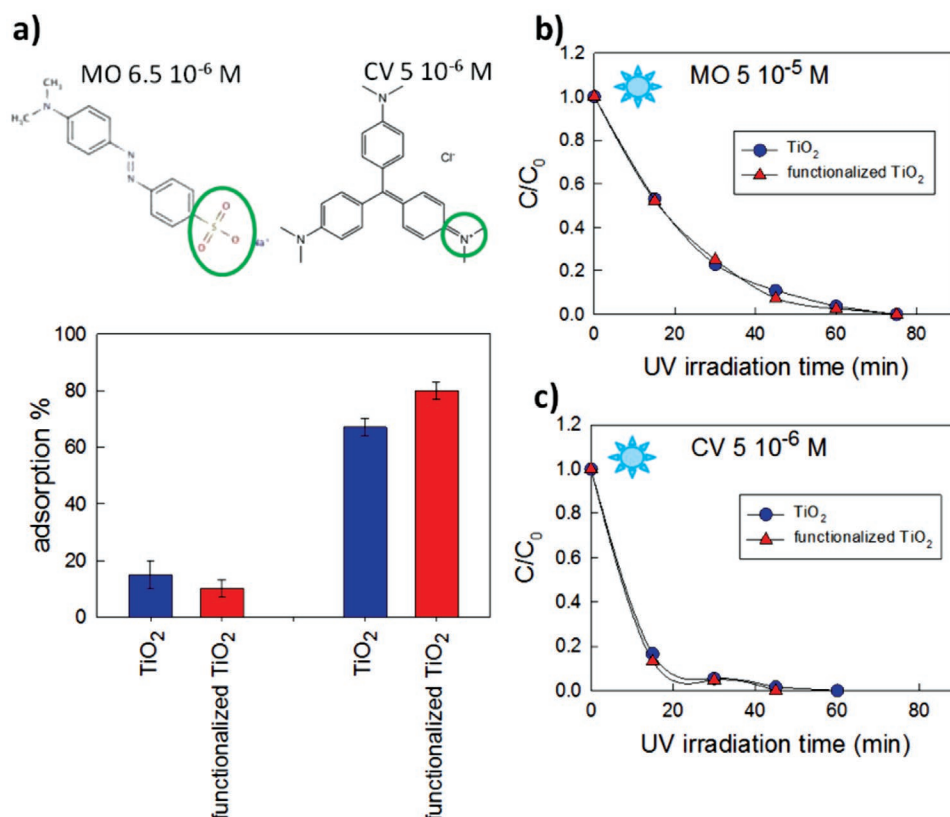


Figure 6. a) Comparison between the absorption capability of TiO₂ beads before and after the functionalization with alginate-derived blend during the interaction with methyl orange 6.5×10^{-6} M and crystal violet 5×10^{-6} M. b) Comparison between the photodegradation activity under UV illumination of TiO₂ beads before and after the functionalization with alginate-derived blend during the interaction with methyl orange 5×10^{-5} M. Error bars included within the experimental point size. c) Comparison between the photodegradation activity under UV illumination of TiO₂ beads before and after the functionalization with alginate-derived blend during the interaction with crystal violet 5×10^{-6} M. Error bars included within the experimental point size.

alginate-derived blend. In fact, the functionalization with alginate-derived slurry enhances the capability of adsorption of MB (from 23% to 82%) and CV (from 67% to 80%), while it is totally ineffective in the enhancement of the adsorption of MO, for which a slight decrease is recorded (from 15% to 10%). This fact would confirm that alginate-derived slurry enhances adsorption of positively charged species through electrostatic interaction, conferring a more negative surface charge to TiO₂ thanks to alginate-derived functional groups. As regards photodegradation (Figure 6b,c), the functionalization with alginate-derived blend enables us to slightly reduce the UV irradiation time needed to obtain complete dye removal in the case of CV (30 instead of 45 min, similarly to what happened in the case of MB) while no effect is observed in the case of MO (75 min). However, the major effect is observed during adsorption.

In order to move toward more complex systems of environmental interest, the degradation of solutions of pharmaceutical micropollutants in mineral water was studied. Both positively and negatively charged pharmaceuticals were investigated: diclofenac (negative) and tetracaine (positive) were chosen as model analytes (Figure S8, Supporting Information). Even if in these cases the percentage of adsorption is lower in comparison to dyes, it is interesting to notice that the functionalization has again positive effects in the case of positively charged pharmaceuticals and detrimental effects in the case of negatively charged

micropollutants (Figure S8a,b for tetracaine and Figure S8c,d for diclofenac in the Supporting Information). In fact, it leads to an enhancement of adsorption (+9%) and reduction of UV irradiation time (−120 min) in the case of tetracaine and it implies a lowering of adsorption (−6%) and an increase of UV irradiation time (+30 min) in the case of diclofenac.

Finally, the photodegradation capability of the TiO₂ system has been studied under visible illumination, using a solar simulator with a power equal to 1 Sun (Figure 7). In this case, 1 g of TiO₂ beads or blend functionalized TiO₂ beads was mixed with 10 mL of MB 6.5×10^{-6} M solution. As shown in Figure 7a, under these conditions the time needed to obtain complete MB degradation is 75 min in the case of not functionalized TiO₂ beads (equal to that under UV illumination) and 60 min for TiO₂ beads functionalized with alginate-derived blend. Both under UV and solar illumination, MB photodegradation follows a first-order kinetics, characterized by rate constants equal to 0.0557 min^{-1} (TiO₂, UV), 0.0458 min^{-1} (TiO₂, solar), 0.134 min^{-1} (functionalized TiO₂, UV), and 0.05 min^{-1} (functionalized TiO₂, solar).

Even if it is known that TiO₂ is a photocatalyst particularly active under UV illumination, it is interesting to note that in the case of macrobeads it is also possible to reach complete MB removal in short time under conditions similar to that of solar illumination. In addition, it has to be underlined that the

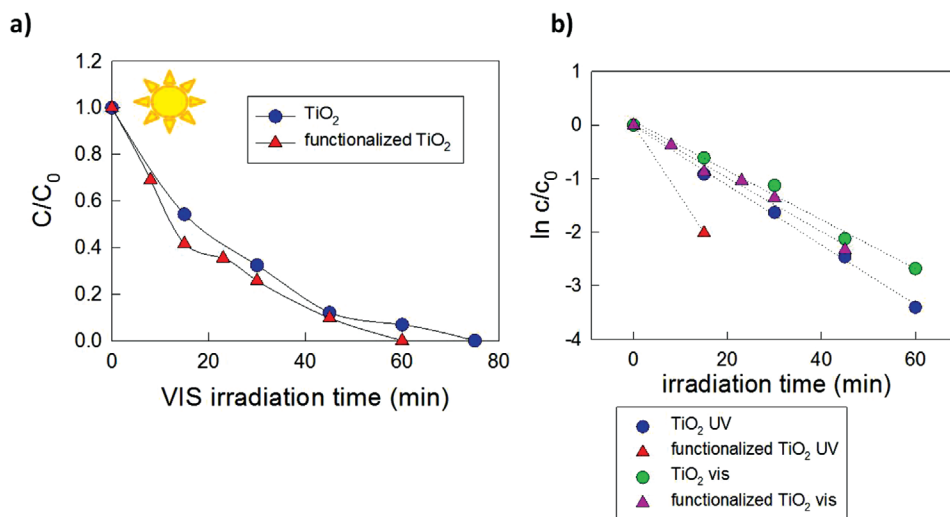


Figure 7. a) Comparison between the photodegradation activity under solar illumination of TiO_2 beads before and after functionalization with alginate-derived blend. MB 6.5×10^{-6} M has been chosen as model pollutant. b) Comparison between the first-order kinetics of TiO_2 beads before and after functionalization with alginate-derived blend during photodegradation under UV and solar illumination of MB 6.5×10^{-6} M solution. Error bars within the experimental point size.

functionalization with alginate-derived blend also improves TiO_2 performances in the spectral range of visible light. The lower effect in comparison to UV illumination can be justified by the fact that alginate-derived C-NPs are characterized by an absorption peak centered at around 300 nm, leading to a maximum interaction with light in the UV region.

3. Conclusion

In this work, we propose novel, environment-friendly substrates for water remediation based on the employment of sodium alginate. This natural, cheap, and biocompatible compound has been used simultaneously as the gelling agent for the preparation of easily recoverable, stable, and porous oxide (TiO_2 , Al_2O_3 , and YSZ) macrobeads, and as a precursor for the preparation of C-NPs containing solution that is utilized to functionalize the oxide beads and improve their decontaminant performances. This active solution has been obtained through a low-energy-demanding process of microwave treatment, without the addition of chemicals (acids or oxidizing agents) in a more environment-friendly way in comparison to conventional hydrothermal synthesis. A similar attention to environmental sustainability has also been paid during the remediation experiments, trying to work in mild conditions, limiting the use of additional chemicals, such as buffers for the control of pH, avoiding heating or complex setups.

These experiments demonstrate that the alginate-derived blend is able to improve adsorption and photodegradation activity of oxide macrobeads. This synergistic effect is intimately related to the complex nature of the active blend, which is a mixture of depolymerized alginate, organic acids, and carbon-based nanoparticles. This multicomponent mixture yields adsorption/photodegradation performances that cannot be reached by functionalizing the beads with the same components taken one by one. We hypothesized that the blend confers

to the macrobeads a more negative surface charge, facilitating the electrostatic interaction with positively charged pollutants, and that the blend components cooperate to create molecular interactions with organic pollutants, thus further enhancing their adsorption.

The functionalization of oxide beads with MW treated alginate solution is a simple universal strategy for water remediation, which enables to overcome the performances of alginate-derived C-Dots synthesized through more complex and more energy-demanding methods, and to obtain a system which is sustainable, eco-friendly, and compatible with circular economy principles.

4. Experimental Section

Synthesis of Oxide Macrobeads: TiO_2 macrobeads were synthesized similarly to what reported by Gijpalaj and Alessandri:^[6] 400 mg of sodium alginate (Sigma Aldrich) was dissolved in 50 mL of Milli-Q (obtained by Milli-Q Integral 5 system) water, together with 100 mg of sodium citrate (Sigma Aldrich). The solution was sonicated in an ultrasound bath for 15 min in order to dissolve completely alginate aggregates, and 8.5 g of TiO_2 nanopowder (Hombikat) was added. The suspension was homogenized by ultrasonication for 30 min and it was added dropwise into the cross-linking solution, previously prepared by dissolving 2.94 g of $CaCl_2 \cdot 2H_2O$ (Sigma Aldrich) in 200 mL of water/ethanol (80/20 vol%) mixture, using a syringe with a needle 23G (0.6 mm) and a dripping velocity of ≈ 0.2 mL s^{-1} . After cross-linking for 24 h, the resulting TiO_2 beads were washed several times with Milli-Q water to remove excessive Ca^{2+} ions and the beads were dried in air. A similar procedure was followed for the synthesis of Al_2O_3 and YSZ ZrO_2 beads, substituting TiO_2 nanopowder with Al_2O_3 (10 g) and YSZ (15 g) nanopowders.

Synthesis and Characterization of Alginate-Derived Active Blend: Alginate-derived active blend was synthesized by dissolving 45 mg of sodium alginate (Sigma Aldrich) in 50 mL of Milli-Q water and treating the solution with a microwave digestion system (CEM Discover Microwave). In particular, the solution was sonicated in an ultrasound bath for 15 min in order to completely dissolve alginate aggregates and treated with the digester, set with the following program: ramp rate, 40 $^\circ C$ min^{-1} ; holding temperature, 200 $^\circ C$; holding time, 15 min; maximum pressure, 200 bar; and power, 150 W.

The resulting solution was characterized by means of UV–vis spectroscopy (QE 65 000 Ocean Optics spectrometer), Raman μ -spectroscopy (Labram HR-800, Horiba Jobin-Yvon, using a He–Ne laser source ($\lambda = 632.8$ nm)), IR spectroscopy (Equinox 55 spectrometer, Bruker), NMR spectroscopy (Bruker Avance 300 MHz Spectrometer), NTA (Nanosight300, Malvern Panalytical), and scanning transmission electron microscopy high-angle annular dark-field imaging (TECNAI F20 high-resolution transmission electron microscope with a scanning-transmission imaging mode and high-angle-annular-dark-field detector). For TEM observation, a drop of suspension was released over a conventional holey-carbon film grid and gently dried at 50 °C for 1 h in air.

As a reference, alginate-derived C-Dots were synthesized following the procedure reported by Zhou et al.^[25] About 250 mg of sodium alginate was dissolved in 10 mL of Milli-Q water and it was sonicated in an ultrasound bath for 15 min, in order to dissolve alginate aggregates; then 2.5 mL of H₂O₂ solution 3 wt% was added. The solution was transferred into a stainless steel autoclave with a Teflon liner with 125 mL capacity. The autoclave was sealed and heated at 220 °C for 12 h. Then, the reactor was allowed to cool at room temperature, and the resulting solution was diluted with Milli-Q water in order to obtain a nominal concentration of alginate equal to that of the aforementioned C-NPs solution.

Functionalization of Oxide Macrobeads: Both carbon-based solutions were utilized to functionalize oxide macrobeads: 300 mg of oxide beads was immersed in 3 mL of solutions and stirred for 60 min. The solution was then removed and the functionalized beads were dried overnight in air.

Evaluation of Decontamination Performances: The performances of Al₂O₃, YSZ, and TiO₂ macrobeads during the removal of different pollutants (methylene blue: 6.5×10^{-6} M; crystal violet: 5×10^{-6} M; methyl orange: 6.5×10^{-6} and 5×10^{-5} M; diclofenac: 1×10^{-4} M; and tetracaine: 9.5×10^{-5} M) were evaluated and compared with those of analogs beads functionalized with alginate-derived active blend. In all the cases, 300 mg of macrobeads was mixed with 3 mL of pollutant solution for 90 min in dark, in order to obtain the adsorption–desorption equilibrium and evaluate the adsorption capability of the system. The suspension was then illuminated with a UV lamp (Philips UV lamp, which emits in the range of 340–410 nm with a maximum at 365 nm, a power of 40 W, and a fluence rate of 71 mJ cm⁻²), in order to determine the system photodegradation capability. All experiments were performed without the addition of any pH buffer (except when differently specified), with constant UV light intensity and distance from the lamp (3 cm). Every 15 min an aliquot was collected, centrifuged, and analyzed by UV–vis spectroscopy, evaluating the variation over the time of the intensity of the absorbance peak of the different analytes.

All the experiments were performed three times, in order to achieve a significant statistics.

For methylene blue, the absorbance variation was calculated at $\lambda = 664$ nm, for methyl orange at $\lambda = 464$ nm and for crystal violet at $\lambda = 588.5$ nm. In the case of diclofenac and tetracaine, samples were analyzed by means of high performance liquid chromatography (HPLC, Dionex UltiMate 3000 Thermo Fisher Scientific) equipped with a UV detector, measuring the absorbance at $\lambda = 275$ nm for diclofenac and at $\lambda = 270$ nm for tetracaine. The percentage of adsorbed pollutant was determined using the following equation

$$\% \text{ adsorbed} = \frac{A_0 - A_t}{A_0} \times 100 \quad (1)$$

where A_0 is the initial value of absorbance of the analyte (proportional to the value of the initial concentration) and A_t is the value of absorbance measured at time t after the mixing in the dark. The absorbance after 90 min of mixing in the dark (A_{90}) was considered as the initial value of absorbance for the photodegradation experiments and utilized for the evaluation of the C_0 of the photodegradation experiments.

Studies regarding the relationship between the adsorption capabilities of the system and the pollutant solution pH were performed using HCl and NaOH to achieve final pH values equal to 1.5 and 11.5, respectively. Studies regarding the relationship between the adsorption capabilities of the system and the adsorbent amount were conducted by suspending

75, 150, or 300 mg of TiO₂ macrobeads in 3 mL of MB solution at pH 6.5. Recyclability tests were performed on 300 mg of macrobeads in 3 mL of MB solution at pH 6.5. Adsorption and photodegradation experiments were performed, at the end of which the remaining water solution was removed and the macrobeads were let dry at room temperature for at least 12 h. Second and third cycles were performed consecutively in the same way.

Experiments under visible illumination were performed using a solar simulator (Abet Technologies, Sun 2000 Simulator, model: 11 016) with an illumination intensity equal to 1 Sun (irradiance: 1.5 A. M., working distance: 15 cm).

Supporting Information

Supporting Information is available from the Wiley Online Library or from the author.

Acknowledgements

This work was carried out with the support of Ministero Italiano delle Politiche Agricole, Alimentari, Forestali e del Turismo (MIPAAFT) in the framework of RESTART project. I.V. and I.A. acknowledge Malvern Panalytical for Nanosight NS300 analysis.

Conflict of Interest

The authors declare no conflict of interest.

Authors Contribution

I.V. synthesized the alginate-derived active blend and performed all the pollutant degradation experiments; J.G. synthesized the oxide macrobeads; S.C. and M.M. performed NMR analysis; A.G. performed HPLC analysis; M.F. performed TEM imaging; and I.A. supervised all the experiments. All authors have given approval to the final version of the manuscript.

Keywords

alginate, C-Dots, oxide beads, photodegradation, pollutant adsorption, water decontamination

Received: October 15, 2019

Revised: February 3, 2020

Published online: April 26, 2020

- [1] I. Vassalini, I. Alessandri, *Catalysts* **2018**, *8*, 569.
- [2] I. Vassalini, I. Alessandri, *Nanoscale* **2017**, *9*, 11446.
- [3] S. Mura, Y. Jiang, I. Vassalini, A. Gianoncelli, I. Alessandri, G. Granozzi, L. Calvillo, N. Senes, S. Enzo, P. Innocenzi, L. Malfatti, *ACS Appl. Nano Mater.* **2018**, *1*, 6724.
- [4] R. Daghrir, P. Drogui, D. Robert, *Ind. Eng. Chem. Res.* **2013**, *52*, 3581.
- [5] H. Dong, G. Zeng, L. Tang, C. Fan, C. Zhang, X. He, Y. He, *Water Res.* **2015**, *79*, 128.
- [6] J. Gijpalaj, I. Alessandri, *J. Environ. Chem. Eng.* **2017**, *5*, 1763.
- [7] G. Orive, S. K. Tam, J. L. Pedraz, J. P. Hallé, *Biomaterials* **2006**, *27*, 3691.
- [8] A. F. Hassan, A. M. Abdel-Mohsen, H. Elhadidy, *Int. J. Biol. Macromol.* **2014**, *68*, 125.

- [9] N. M. Mahmoodi, B. Hayati, M. Arami, H. Bahrami, *Desalination* **2011**, 275, 93.
- [10] S. Thakur, S. Pandey, O. A. Arotiba, *Carbohydr. Polym.* **2016**, 153, 34.
- [11] S. Asadi, S. Eris, S. Azizian, *ACS Omega* **2018**, 3, 15140.
- [12] Y. Wang, W. Wang, A. Wang, *Chem. Eng. J.* **2013**, 228, 132.
- [13] L. Wang, C. Cheng, S. Tapas, J. Lei, M. Matsuoka, J. Zhang, F. Zhang, *J. Mater. Chem. A* **2015**, 3, 13357.
- [14] W. Shi, F. Guo, H. Wang, C. Liu, Y. Fu, S. Yuan, H. Huang, Y. Liu, Z. Kang, *Appl. Surf. Sci.* **2018**, 433, 790.
- [15] H. Zhang, L. Zhao, F. Geng, L. H. Guo, B. Wan, Y. Yang, *Appl. Catal., B* **2016**, 180, 656.
- [16] C. Cheng, D. Lu, B. Shen, Y. Liu, J. Lei, L. Wang, J. Zhang, M. Matsuoka, *Microporous Mesoporous Mater.* **2016**, 226, 79.
- [17] R. K. Das, J. P. Kar, S. Mohapatra, *Ind. Eng. Chem. Res.* **2016**, 55, 5902.
- [18] Q. Lu, Y. Zhang, S. Liu, *J. Mater. Chem. A* **2015**, 3, 8552.
- [19] H. Bozetine, Q. Wang, A. Barras, M. Li, T. Hadjersi, S. Szunerits, R. Boukherroub, *J. Colloid Interface Sci.* **2016**, 465, 286.
- [20] R. Liu, H. Li, L. Duan, H. Shen, Y. Zhang, X. Zhao, *Ceram. Int.* **2017**, 43, 8648.
- [21] H. Li, X. He, Z. Kang, H. Huang, Y. Liu, J. Liu, S. Lian, C. H. A. Tsang, X. Yang, S. T. Lee, *Angew. Chem., Int. Ed.* **2010**, 49, 4430.
- [22] A. Bhati, S. R. Anand, G. Gunture, A. K. Garg, P. Khare, S. K. Sonkar, *ACS Sustainable Chem. Eng.* **2018**, 6, 9246.
- [23] H. Safardoust-Hojaghan, M. Salavati-Niasari, *J. Cleaner Prod.* **2017**, 148, 31.
- [24] Y. Shin, J. Park, D. Hyun, J. Yang, J. H. Lee, J. H. Kim, H. Lee, *Nanoscale* **2015**, 7, 5633.
- [25] J. Zhou, W. Deng, Y. Wang, X. Cao, J. Chen, Q. Wang, W. Xu, P. Du, Q. Yu, J. Chen, M. Spector, J. Yu, X. Xu, *Acta Biomater.* **2016**, 42, 209.
- [26] P. Atienzar, A. Primo, C. Lavorato, R. Molinari, H. García, *Langmuir* **2013**, 29, 6141.
- [27] A. Prasannan, T. Imae, *Ind. Eng. Chem. Res.* **2013**, 52, 15673.
- [28] A. Konwar, U. Baruah, M. J. Deka, A. A. Hussain, S. R. Haque, A. R. Pal, D. Chowdhury, *ACS Sustainable Chem. Eng.* **2017**, 5, 11645.
- [29] A. Konwar, D. Chowdhury, *RSC Adv.* **2015**, 5, 62864.
- [30] M. Algarra, L. Dos Orfãos, C. S. Alves, R. Moreno-Tost, M. S. Pino-González, J. Jiménez-Jiménez, E. Rodríguez-Castellón, D. Eliche-Quesada, E. Castro, R. Luque, *ACS Sustainable Chem. Eng.* **2019**, 7, 10493.
- [31] Z. Zhang, W. Sun, P. Wu, *ACS Sustainable Chem. Eng.* **2015**, 3, 1412.
- [32] R. Miao, Z. Luo, W. Zhong, S. Y. Chen, T. Jiang, B. Dutta, Y. Nasr, Y. Zhang, S. L. Suib, *Appl. Catal., B* **2016**, 189, 26.
- [33] S. Majumdar, G. Krishnatreya, N. Gogoi, D. Thakur, D. Chowdhury, *ACS Appl. Mater. Interfaces* **2016**, 8, 34179.
- [34] D. Rodríguez-Padrón, M. Algarra, L. A. C. Tarelho, J. Frade, A. Franco, G. De Miguel, J. Jiménez, E. Rodríguez-Castellón, R. Luque, *ACS Sustainable Chem. Eng.* **2018**, 6, 7200.
- [35] E. Liu, D. Li, X. Zhou, G. Zhou, H. Xiao, D. Zhou, P. Tian, R. Guo, S. Qu, *ACS Sustainable Chem. Eng.* **2019**, 7, 9301.
- [36] L. Wang, M. Li, W. Li, Y. Han, Y. Liu, Z. Li, B. Zhang, D. Pan, *ACS Sustainable Chem. Eng.* **2018**, 6, 12668.
- [37] V. Ramanan, S. K. Thiyagarajan, K. Raji, R. Suresh, R. Sekar, P. Ramamurthy, *ACS Sustainable Chem. Eng.* **2016**, 4, 4724.
- [38] D. Sarma, B. Majumdar, T. K. Sarma, *ACS Sustainable Chem. Eng.* **2018**, 6, 16573.
- [39] S. Zhang, H. Yang, H. Huang, H. Gao, X. Wang, R. Cao, J. Li, X. Xu, X. Wang, *J. Mater. Chem. A* **2017**, 5, 15913.
- [40] S. Singh, N. Shauloff, R. Jelinek, *ACS Sustainable Chem. Eng.* **2019**, 7, 15.
- [41] S. Mao, T. Zhang, W. Sun, X. Ren, *Pharm. Dev. Technol.* **2012**, 17, 763.
- [42] T. M. Aida, T. Yamagata, M. Watanabe, R. L. Smith, *Carbohydr. Polym.* **2010**, 80, 296.
- [43] T. M. Aida, T. Yamagata, C. Abe, H. Kawanami, M. Watanabe, R. L. Smith, *J. Supercrit. Fluids* **2012**, 65, 39.